

^3He - ^4He mixtures in two dimensions*

M. D. Miller

Department of Physics and Astronomy, University of Massachusetts, Amherst, Massachusetts 01003

(Received 21 July 1977)

In this paper we discuss the thermodynamic properties of a physisorbed mixture of ^3He and ^4He . We present microscopic calculations of the zero-temperature liquid-gas and phase-separation aspects and extend these results to finite temperature, in an approximate way, using a simple model. The results are then compared to the recent experimental data of Hickernell, McLean, and Vilches on ^3He - ^4He mixtures on graphite. We conclude that the low-density phases of ^3He - ^4He on graphite are *not* well understood and in particular the identification of the major structures in the experimental data as the liquid-gas transition is not straightforward.

I. INTRODUCTION

Experimental studies of mixtures of ^3He and ^4He in bulk liquid,¹ solid,² and physisorbed films³ have provided a wealth of information concerning the behavior of strongly correlated quantum systems. Hickernell, McLean, and Vilches⁴ (HMV) have recently reported a heat-capacity study of the isotopic mixture as physisorbed *submonolayers*. The HMV results were surprising since they found no clear evidence of phase separation; that is, except for a small broad shoulder which appeared at small ^3He concentrations and *disappeared* with increasing concentration, all the features evolved smoothly out of the pure phases. The most prominent specific-heat peak (which appears from the ^4He side at temperatures ~ 1 K) has most recently been interpreted as the liquid-gas phase transition.⁵ The magnitude of this peak (at a given areal density) decreases with increasing ^3He concentration x and disappears for $x > 0.5$. The ^3He -rich side is basically featureless except for a small broad peak ~ 80 mK.

In this paper we will describe a theory of the liquid-gas and phase-separation aspects of this mixture. Because a first-principles approach to these phase transitions is, at present, out of reach, the starting point of the analysis will be the zero-temperature equations of state obtained from a variational calculation. The basic approximation of the zero-temperature calculation is that an accurate description of the adsorbed system is obtained by dividing the physics into a two-dimensional (2D) many-body problem and a one-dimensional (1D) one-body problem. This approximation will be discussed and explained in Sec. II. In Sec. III the details of the $T=0$ K calculation will be presented: this will include a description of the statistical cluster expansion as adopted for the mixture. In Sec. IV we shall present and discuss the results of the zero-temperature calculation. We shall then presume the finite-temperature behavior by use of simple

models and inference gleaned from our experience with the bulk. Finally we shall compare theory with HMV in order to try to draw some conclusions concerning the present extent of our understanding of the physics of low-density adsorbed He submonolayers.

II. ADSORBED He ON GRAPHITE

The substrate used by HMV (a commercial form of exfoliated graphite) appears, from studies of the pure phases,^{6,7} to provide a reasonably uniform surface whose physisorbed states are quasi-two-dimensional in character. The periodicity of the graphite substrate induces a band structure in the adsorbate; however, at low coverages the band widths are wide and the band gaps are narrow⁸ and so in excellent approximation the substrate can be simply thought of as a source of *uniform* external potential. For the graphite substrate, the potential well seen by a He atom is very deep (~ -250 K) and so the adatom finds itself locked into a rigid two-dimensional plane (e.g., the first excited single-particle state is ~ 80 K higher than the ground state). In this limit then the physics of the adsorbed system is separable into two parts: one which concerns directions perpendicular to the substrate surface (the z axis, with the substrate occupying the negative $-z$ half-space) and the other which concerns those directions parallel to the plane of the substrate surface. This convenient division of the problem into a 2D many-body problem coupled with a 1D single-particle problem was first applied to ^4He submonolayers by Jackson⁹ and has yielded reasonable agreement between the calculated and experimental low-temperature specific heats.¹⁰ It is clearly attractive to extend this model to the mixture. That this is indeed reasonable is illustrated by Fig. 1 where we show the ground state single-particle probability densities for atoms of ^3He and ^4He . It is evident that not only are

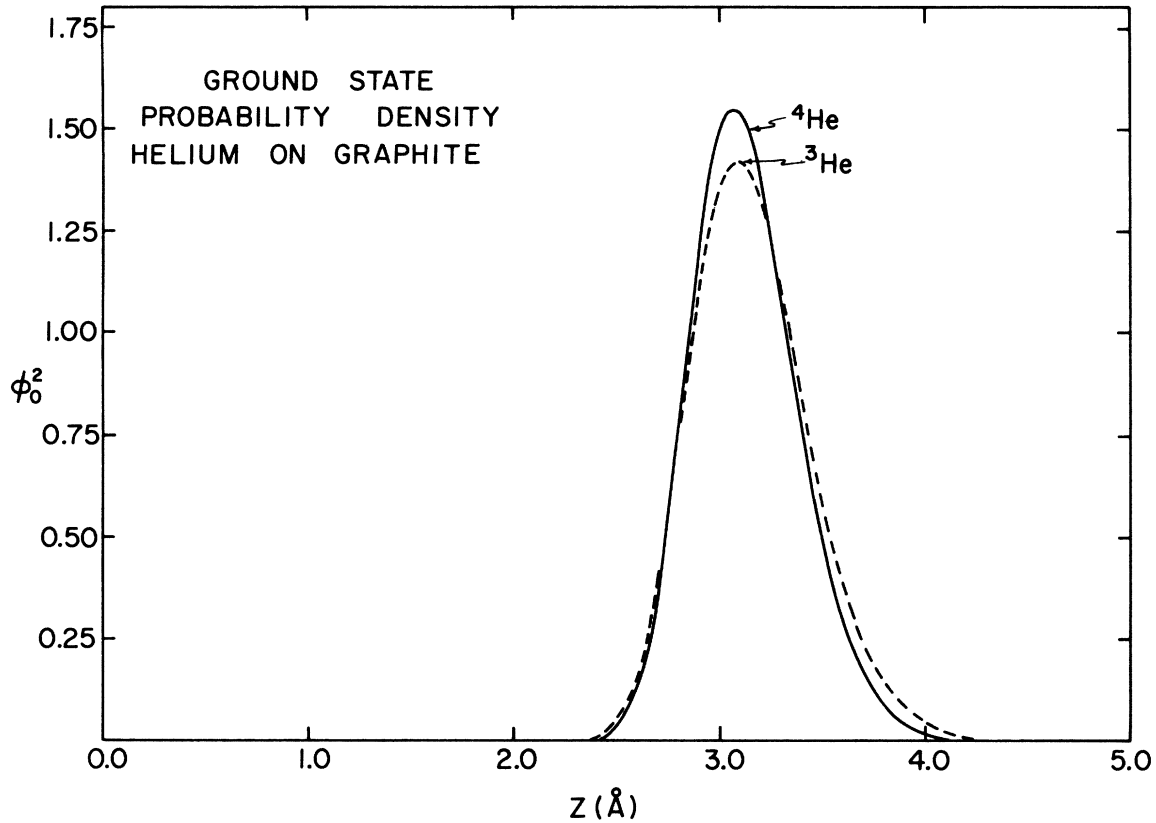


FIG. 1. Ground-state single-particle probability densities for ^3He and ^4He on graphite. The He atoms are well localized in the same plane $\sim 3 \text{ \AA}$ above the substrate.

the atoms well localized above the substrate surface but, as importantly, they peak at about the same z value (i.e., the ^3He and ^4He systems are in the *same* plane). Because the energy difference between the z excited states and the z ground state is large compared to the relevant temperatures the excited states will be relatively unpopulated and will make an unimportant contribution to the thermodynamics. Thus in the following we shall only consider the 2D many-body problem as determining the thermodynamic state. This approximation will be further discussed in Sec. IV.

III. THEORY OF ^3He - ^4He MIXTURES

We consider a 2D mixture of xN ^3He atoms and $(1-x)N$ ^4He atoms interacting with a Lennard-Jones potential

$$V(r) = 4\epsilon[(\sigma/r)^{12} - (\sigma/r)^6] \quad (1)$$

$$\epsilon = 10.22\text{K}, \quad \sigma = 2.556 \text{ \AA} .$$

The energy per particle is calculated variationally using a Slater-Jastrow wave function ψ_{SJ} ,

$$\psi_{\text{SJ}} \equiv \Phi F = \alpha \left[\prod_{j=1}^{N_3} e^{i\vec{k}_j \cdot \vec{r}_j} \xi(m_j) \right] \prod_{1 \leq i < j \leq N} f(r_{ij}) \quad (2)$$

where α is the antisymmetrizer for the N_3 fermion labels, $\xi(m_j)$ is the spin function for the j th particle, and the pair factor f is given by

$$f_{\alpha\beta}(r) = e^{u_{\alpha\beta}(r)/2} = e^{-(b_{\alpha\beta}\sigma/r)^{5/2}} \quad (3)$$

In Eq. (3), $b_{\alpha\beta}$ is a variational parameter and the $(\alpha, \beta) = (3, 4)$ indicates that a different function can be chosen for each type of pair.¹¹

The Hamiltonian for the mixture H is given by

$$H = -\frac{\hbar^2}{2m_3} \sum_{i=1}^{N_3} \nabla_i^2 - \frac{\hbar^2}{2m_4} \sum_{i=1}^{N_4} \nabla_i^2 + \sum_{i < j} V(r_{ij}) \quad (4)$$

Using ψ_{SJ} , then, the energy expectation value E can be cast in the form

$$E = (1-x)^2 E_{44}(x) + 2x(1-x) E_{34}(x) + x^2 \left[E_{33}(x) + \sum_{F=1}^{N_3} E_F(x) \right], \quad (5)$$

where the $E_{\alpha\beta}$ are defined as

$$E_{\alpha\beta}(x) = \frac{1}{2} \rho \int g_{\alpha\beta}(r) \bar{V}_{\alpha\beta}(r) d\bar{r} \quad (6)$$

and

$$\bar{V}_{\alpha\beta} = V(r) - \frac{1}{8} \hbar^2 (1/m_\alpha + 1/m_\beta) \nabla^2 u_{\alpha\beta}(r). \quad (7)$$

Also in Eq. (6), ρ is the (areal) number density and the $g_{\alpha\beta}(r)$ are mixed two-particle distribution functions defined by

$$g_{\alpha\beta}(r_{ij}) = \frac{N_\alpha(N_\beta - \delta_{\alpha\beta})}{\rho_\alpha \rho_\beta} \times \int \psi_{Sj}^* \psi_{Sj} d\bar{r}_{(i,j)}^N / \int |\psi_{Sj}|^2 d\bar{r}^N, \quad (8)$$

where ρ_α (ρ_β) is the partial density of species α (β), the notation in the numerator integral indicates that label i and j are not to be integrated over where $i \in \{\alpha\}$ and $j \in \{\beta\}$. The terms denoted by $E_F(x)$ are the cluster expansion form of part of the kinetic energy, viz.,

$$x^2 \sum_{F=1}^{N_3} E_F(x) = \frac{\hbar^2}{4m_3 N} \sum_{i=1}^{N_3} \left(k_i^2 + \int F^2(\bar{\nabla}_i \Phi^* \cdot \bar{\nabla}_i \Phi) / \int |\psi_{Sj}|^2 d\bar{r}^N \right), \quad (9)$$

where F and Φ are defined in Eq. (2). The radial distribution functions $g_{\alpha\beta}$ and the kinetic energy, Eq. (9), are evaluated by means of a straightforward generalization of the usual Wu-Feenberg¹² statistical cluster expansion. The differences in the cluster expansion are due to ψ_{Sj} now mixing boson labels with the fermion labels. For example, two ${}^4\text{He}$ atoms can "see" one another through intermediary ${}^3\text{He}$ atoms as well as ${}^4\text{He}$'s and whenever there are two or more ${}^3\text{He}$'s in the intermediate state they must be antisymmetrized. The distribution functions can be written in the form

$$g_{\alpha\beta}(r) = g_{\alpha\beta}^B(r) + \Sigma_{\alpha\beta}(r) \quad \alpha, \beta = 3, 4, \quad (10)$$

where $g_{\alpha\beta}^B(r)$ is the distribution function generated by F^2 only and Σ represents the statistical cluster expansion contributions. The Wu-Feenberg expansion suffers from the problem of not having a readily available small parameter with which to order the terms.¹³ This problem is enhanced in the mixture since the number of correlated particles is typically not the same number which are being exchanged. However, for

definiteness, we shall choose to order the series by the number of distinct labels in the multiplicative approximants.¹⁴ Roughly speaking this is a density expansion since a term with m number of labels will involve an m -particle distribution function (whose origin is the numerator of that multiplicative approximant). However, the situation is made indistinct because of the concomitant denominator expansion in powers of $1/N$ which introduces the lower distribution functions into each order.

For the purpose of numerical calculations we use a single variational parameter independent of the type of pair and the cluster series has been truncated after the two-body terms. b is, however, density and concentration dependent. In addition we note that, in 2D, in the zero-density limit b is independent of mass or statistics (from dimensional analysis). Thus, for the low-density systems in which we are interested a single variational parameter should suffice. In this approximation then

$$g_{44}(r) \approx g_B(r), \quad g_{34}(r) \approx g_B(r), \quad g_{33}(r) \approx g_B(r) \left[1 - \frac{1}{2} \left(\frac{2J_1(k_F r)}{k_F r} \right)^2 \right], \quad (11)$$

where $k_F = (2\pi\rho x)^{1/2}$ is the Fermi momentum, J_1 is a Bessel function and it should be stressed that the $g_B(r)$ are x dependent. [Because we only use a single b the notation $g_B(r)$ is unambiguous.] Σ_{34} and Σ_{44} make no contribution since they first enter at the three-body level.¹⁵ The same truncation is applied to the kinetic energy, Eq. (9), where we find

$$E_1 = (\hbar^2/2m_3) \pi \rho, \quad (12)$$

$$E_2 = E_1 \frac{32x\rho}{(2\pi)} \int d\bar{r} [g_B(r) - 1] \times \int_0^1 dy J_0(2k_F r y) \times [y^2 \cos^{-1}(y) - y(1-y^2)^{1/2}] y^3, \quad (13)$$

where J_0 is a Bessel function. Thus, for a given $g_B(r)$, Eqs. (11)–(13) allow us to calculate the energy, Eq. (5). We choose to use $g_B(r)$'s which are solutions of the Born-Bogoliubov-Green-Kirkwood-Yvon (BBGKY) equation

$$\bar{\nabla}_1 g_B(r_{12}) = \bar{\nabla}_1 u(r_{12}) g_B(r_{12}) + \rho \int \bar{\nabla}_1 u(r_{13}) g^{(3)}(1, 2, 3) d\bar{r}_3, \quad (14)$$

with the Kirkwood-superposition approximation (KSA) used for the three-body distribution function

$$g^{(3)}(1, 2, 3) \approx g_B(r_{12}) g_B(r_{23}) g_B(r_{31}). \quad (15)$$

The solutions of the BBGKY-KSA have been dis-

cussed for the case of 2D ^4He ,¹⁶ where it was found that they yield results in excellent agreement with molecular dynamics.

For a mixture, all combinations of concentration, pressure (denoted by ϕ), and temperature might not represent states of material stability. If the system separates into two phases then these phases must have the same ϕ , T , and chemical potentials μ_3 and μ_4 . At zero temperature the chemical potentials can be obtained from¹⁷

$$\mu_3 = H + (1-x) \left(\frac{\partial H}{\partial x} \right)_\phi, \quad (16)$$

$$\mu_4 = H - x \left(\frac{\partial H}{\partial x} \right)_\phi, \quad (17)$$

where $H = E + \phi/\rho$ is the enthalpy per particle. It is clear that in order to obtain accurate chemical potentials one needs to have accurate pressures. If one had to obtain ϕ through numerical differentiation of $E(\rho)$ a serious source of error would be present. However, for a system with a power-law potential and a power law $u(r)$, one can show that the virial-theorem pressure, which is given by

$$\phi = \frac{2}{3} \rho (\epsilon_{KE} - 3\epsilon_6 + 6\epsilon_{12}), \quad (18)$$

(where the ϵ 's are the constituents of the energy, $E = \epsilon_{KE} - \epsilon_6 + \epsilon_{12}$), is equal to that obtained by differentiating the energy.¹⁸ Thus, only the derivatives with respect to concentration of Eqs. (16) and (17) have to be obtained numerically. In principle, one could analyze the mixture at fixed density, however, in practice it would prove quite formidable. If the system phase separates at two concentrations x_1 and x_2 ($\neq 0, 1$), then Eqs. (16) and (17) yield

$$H' = [H(x_1) - H(x_2)] / (x_1 - x_2), \quad (19)$$

where

$$H' \equiv \left(\frac{\partial H}{\partial x} \right)_{x_1} = \left(\frac{\partial H}{\partial x} \right)_{x_2}. \quad (20)$$

Equations (19) and (20) are the well-known "double-tangent" construction.

In Sec. IV, we shall discuss the thermodynamic results of solving Eqs. (5), (16), and (17) and examine their role in interpreting the experimental data of HMV.

IV. RESULTS AND DISCUSSION

The results of the energy calculation are shown in Fig. 2. In the inset, we show the energy as a function of density for a given x . The important point in this figure is that whereas 2D ^4He is a liquid, 2D ^3He is a gas. At zero pressure, ^3He is at zero density. Thus,

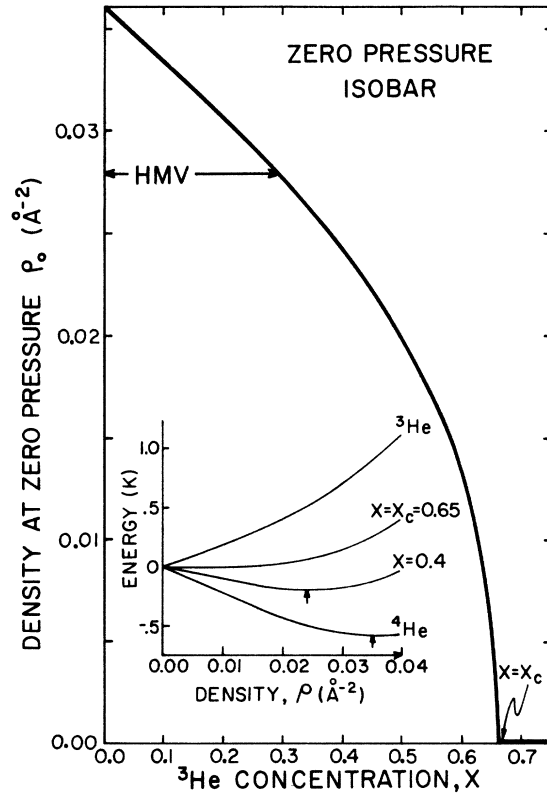


FIG. 2. In the inset we show the energy as a function of (areal) density for various ^3He concentrations. In the main figure we show the density at zero-pressure as a function of concentration from which we can read off $x_c = 0.65$. The arrow labeled HMV is the position of the lowest-density system studied by HMV.

in contrast with the bulk the 2D system is a liquid-gas mixture. The consequence is that phase-separation and the liquid-gas transition become intermingled and each must be discussed in the light of the other. We begin with the liquid-gas transition.

We see, from Fig. 2 that the energy, at fixed density, increases monotonically with increasing x . We can thus find a concentration x_c , which separates those mixtures which have an energy minimum at finite density, $x < x_c$, from those whose minimum occurs at zero-density, $x \geq x_c$. The value for x_c can be read off of Fig. 2 where we show the density at zero pressure ρ_0 , since x_c is determined by the $\rho_0 = 0.0$ intercept. We find $x_c \approx 0.65$. Because x_c is determined at zero density its value can also be obtained analytically through a density expansion of the energy, Eq. (5). We then find x_c to be a solution of the quadratic equation

$$(5\eta_{CB} - \eta_3)x_c^2 + 10(\eta_3 - \eta_4)x_c - 10(\eta_{CB} - \eta_4) = 0, \quad (21)$$

where we have defined the following quantities:

$$\begin{aligned}\eta_3 &= (h^2/m_3\epsilon\sigma^2) = 0.2409, \\ \eta_4 &= (h^2/m_4\epsilon\sigma^2) = 0.1815, \\ \eta_{CB} &= \left(\frac{24}{25}\right)\left[\frac{1}{2}\Gamma\left(\frac{9}{5}\right)\right]^{5/3} = 0.2686.\end{aligned}\quad (22)$$

Drawing from these ground-state results we can develop a model for the liquid-gas transition in the mixture. Pure 2D ^4He has a liquid ground state and so, if we can extrapolate from the bulk, there will be a liquid-gas coexistence line in the ϕ - T plane terminating at a critical point ($x=0, \phi_{4c}, T_{4c}$). If we add ^3He to the system then it should become "easier" to induce a transition since the ^3He component is itself unbound. Thus, with increasing x , the critical point and coexistence line should move to lower temperatures and pressures and so we can envision a critical locus beginning at ($x=0, \phi_{4c}, T_{4c}$), terminating at ($x=x_c, \phi_c=0, T_c=0$), which when taken together with the ^4He coexistence line and that portion of the x axis, for which $x \leq x_c$, form the boundary of a triangular "canopy" in (x, ϕ, T) space: the liquid-gas coexistence surface (LGCS). The specific-heat signature which one obtains by encountering the LGCS is then a series of peaks which move to decreasing temperature with decreasing density, for a given density they move to lower temperatures with increasing x , and finally there should be *no* peaks for $x > x_c$ ($=0.65$). This pattern basically describes the 1-K "anomalies" of HMV except that the HMV peaks disappear by $x \approx 0.5$ (the type of discrepancy which can be ascribed to substrate inhomogeneity). Unfortunately, this agreement does not really *prove* anything. If peaks were present in the HMV data for $x > 0.65$ that would be devastating for this liquid-gas model, however, the fact that the amplitude disappears smoothly with increasing x is entirely reasonable behavior for practically any reason for which ^4He would have a peak and ^3He would not.

There is, in fact, an important discrepancy between the ground-state calculations and the interpretation of the HMV peaks as the liquid-gas transition. The HMV data certainly must represent that part of liquid-gas coexistence for which the density is *less* than the critical density. The densities ρ_0 shown in Fig. 2, however, represent the *maximum* density points on the saturation curves (i.e., equilibrium at $T=0$ K between a liquid- and zero-density gas). Thus, for pure ^4He , for example, $\rho_0=0.036 \text{ \AA}^{-2}$, however, the HMV data is still moving to *increasing* temperature at 0.048 \AA^{-2} , as is shown in Fig. 3. This variance in the densities is impressive and reconciling them is quite despairing. Two possible problem areas for the calculation present themselves: (i) the calculated values of ρ_0 could be quite inaccurate. In 2D, the kinetic and potential energy cancellation is much more complete than in the bulk¹⁹ (3.0–3.6 K compared to 11.5–17.5 K), which can make ρ_0 strongly dependent on the par-

ticular potential function²⁰ or model wave function. In the bulk, the calculated ρ_0 's tend to be smaller than their measured values. (ii) Band effects due to the periodic substrate potential could make the adatoms behave as if they had an effective mass. Thus, for example, if $m_{\text{eff}} \approx 1.3m_4$, the ρ_0 would be increased to $\sim 0.06 \text{ \AA}^{-2}$. However, the calculation of the band structure⁸ and the calculation of the many-body ground state including the band structure²⁰ seem to indicate that the periodicity of the substrate potential has negligible effects for low-density He on graphite. Finally, we note the distinct possibility that the HMV peaks are not due directly to the liquid-gas phase transition. We shall return to these points after the following discussion of phase separation in the mixture.

In Fig. 4 we show $\mu_3 - \mu_4$ ($=\partial H/\partial x$) as a function of x . For the existence of an (upper) critical solution point it is necessary that $\partial^2 H/\partial x^2 < 0$ over some range of x .¹⁷ At the lower pressures shown in Fig. 4, H , undergoes regions of changing curvature which induce phase separation (the boundaries of the two-phase region are denoted by circles). At the largest pressure $\partial^2 H/\partial x^2 > 0$ for all x and there is no separation. We note in passing that the $x=0$ intercepts are one-third the ^4He kinetic energy (at that pressure) as first pointed out by Baym.²¹ This is easily obtained by calculating $\lim_{x \rightarrow 0} (\partial E/\partial x)$ from Eq. (5), [that is, $(\partial E/\partial x)_p = (\partial H/\partial x)_\phi$].

After a detailed analysis of μ_3 and μ_4 (the "double-tangent" construction), we obtain the phase-separation curve shown in Fig. 5. At the lowest pressures the system separates into pure ^3He and ^4He phases. With increasing pressure, ^3He becomes soluble in ^4He and for $\phi > 0.045 \text{ dyn/cm}$ there is only one phase. Thus,

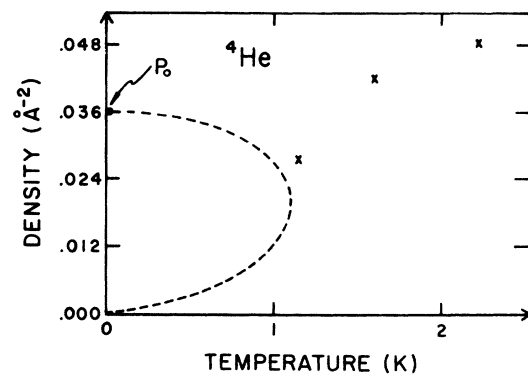


FIG. 3. Density as a function of temperature for pure ^4He where we show the *calculated* zero-pressure density ρ_0 compared with the HMV data (x 's). The HMV data are the positions of the maxima in the specific heat curves. The dashed line showing the extent of the liquid-gas two-phase region was drawn to an arbitrary critical temperature and is meant to be only a guide to the typical shape expected for such a region.

at zero temperature for low enough pressure the system will phase separate.

In order to discuss the relationship between phase separation and the LGCS in a more quantitative way we will use a simple model to fill out the finite temperature behavior of the phase-separation surface. Let us construct an approximate Gibbs free energy of mixing²² from the zero-temperature enthalpy of mixing and the entropy of mixing S_M for an ideal solution, where $S_M = -x \ln x - (1-x) \ln(1-x)$.²³ In Fig. 6 we show the behavior of the critical solution points which are obtained from this model. For $\rho_c = 0.0$, we find $x = x_c$ and as ρ_c increases the critical point moves to larger x and smaller T_c . These results are clearly what one would have surmised from inspection of the zero-temperature "footprint," Fig. 5. The fact that $dT_c/d\phi$ is large and negative is due to the large excess area in the liquid-gas mixture (from regular solution theory).

If we now combine the liquid-gas and phase-separation results, we find two types of regions depending on whether or not the LGCS and phase-separation surface intersect. In Fig. 7 we show these two possibilities, very schematically, as cuts in a (T, x) plane at fixed pressure. At very low pressures we expect to find the situation of Fig. 7(a) where the liquid-gas line intersects the phase-separation region at, in this case, a tricritical point. Thus, at low pressures, we expect a binary phase equilibrium between a ^4He -rich liquid and a ^3He -rich vapor. At higher pressures, Fig. 7(b), the surfaces will no longer meet and so there will be two critical points and a region of a homogeneous mixed phase.

If one does a constant-area small- x specific-heat measurement of the mixture as shown in Fig. 7(a)

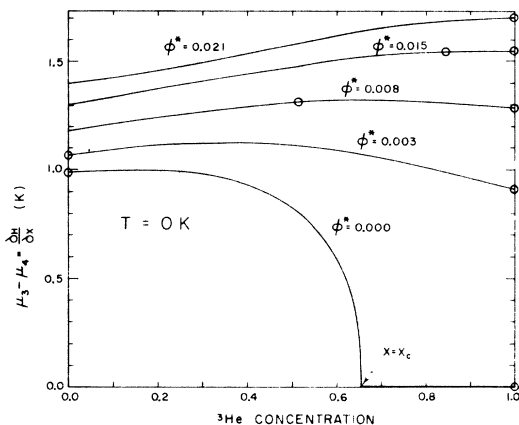


FIG. 4. Difference in the chemical potentials $\mu_3 - \mu_4 = \partial H / \partial x$ as a function of x for various reduced pressures. [For pressures in dyn/cm multiply the reduced pressures ϕ^* ($\equiv \phi \sigma^2 / \epsilon$) by 2.16.] The circles denote the boundaries of the two-phase region.

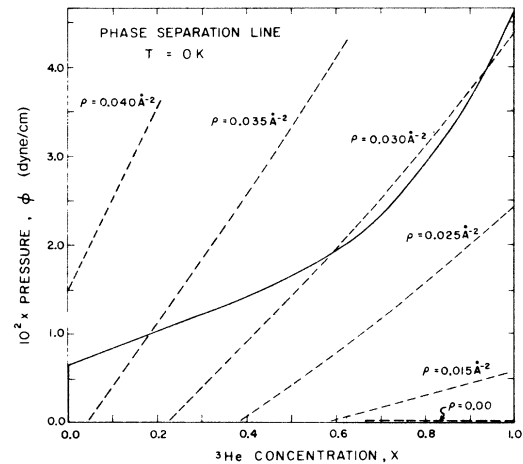


FIG. 5. Phase-separation curve locating the two-phase region at zero temperature. The isochores show that for densities greater than $\sim 0.04 \text{ \AA}^{-2}$ the system will not phase separate.

then one will *not* find a two-peak signature since the system will simply "slide" down the liquid-gas surface until it encounters the phase separation region. At large x ($x > 0.65$) from both Figs. 7(a) and 7(b), phase-separation peaks should be observed in the mixture. This structure is not found in the data of HMV.

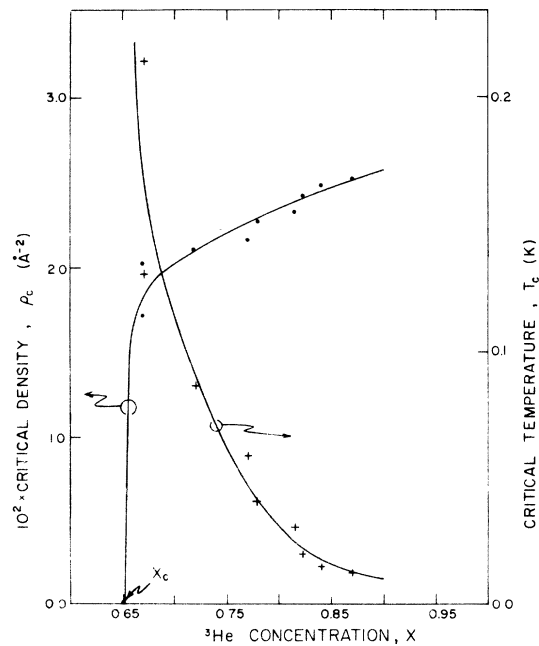


FIG. 6. Behavior of the line of critical solution points using the simple finite temperature approximation described in the text. The line moves to increasing density and decreasing temperature with increasing ^3He concentration.

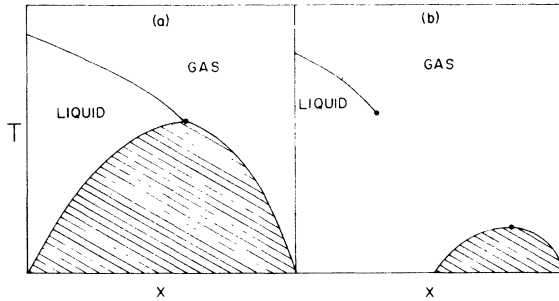


FIG. 7. Schematic look at the combined liquid-gas and phase-separation properties for $^3\text{He}-^4\text{He}$ mixtures. (a) The situation at low pressure and (b) at higher pressure.

The absence of phase-separation peaks (for $x > x_c$) taken together with the density problems, discussed above, constitute a serious problem in relating the microscope calculations to the HMV data. Every calculation which has been done on the ^4He ground state has reinforced the conclusion that it is a self-bound system. The calculation of Novaco and Campbell²⁰ which used a more general form for the trial function and a Beck potential indeed found precisely the same ρ_0 as reported here for ψ_{SJ} and a Lennard-Jones potential. Schick and Campbell²⁴ found that a substrate-mediated phonon interaction would tend to enhance the binding (although the influence on ρ_0 is not known). In addition, the nature of many-body binding for 2D ^3He and ^4He has also been confirmed by use of the quantum theorem of corresponding states.²⁵ The ground-states thermodynamic phases of pure 2D ^3He and ^4He seem, from a theoretical point of view, to be firmly established. The question of phase-separation is on less sure footing since phase-separation does not depend on the particular state of the *pure* phases but is a stability question with respect to changes in concentration. However, for the 2D $^3\text{He}-^4\text{He}$ system, the *extent* of phase separation appears to be more model dependent (i.e., choice of wave function, potential, method of evaluating expectation values, etc.) than its existence. At zero-pressure the energy increases monotonically from $x=0$ to $x=x_c$ with basically negative curvature (cf. Fig. 4). If this behavior is not due to some approximation, then, since one can bound such a curve from below with a line between $-|E_4|$ (at $x=0$) to 0.0 (at $x=1$), such a system will phase separate. (The question as to what sort of systems tend to phase separate has been investigated for a general class of boson-fermion mixtures using a corresponding states type of approach and will be published elsewhere.)

One possibility of explaining the differences between theory and HMV is that the periodic substrate potential has not been given its due. The HMV peaks (the 1-K structure) thus, for example, might represent

super lattice structure other than the $\sqrt{3} \times \sqrt{3}$ or they could be a sublimationlike coexistence region between the low-density solid and a gas. It seems unlikely, however, that these models could explain the flagrant isotopic dependence exhibited by the peaks especially in light of the rather mild isotopic differences in the $\sqrt{3} \times \sqrt{3}$ phase.⁴ A final possibility is that these peaks *are* the liquid-gas transition (or at least its manifestation) which has been distorted from its pure 2D behavior by the external field. However, this model, as illustrated in Fig. 8 for pure ^4He would seem to require a liquid "island" placed between the low-density gas and the registered phase for which there is no experimental justification (there would be a low-density triple point).

In conclusion then, the low-density phases of adsorbed He on graphite are not well understood. It should also be pointed out that the nature of the phase for densities just greater than the registered phase is not known.²⁶

ACKNOWLEDGMENTS

I would like to thank Professor L. H. Nosanow with whom this work was begun and whose ideas initiated the research and Professor R. A. Guyer, whose many critical comments brought some order into the chaos. In addition, I would like to thank Professor J. G. Dash, Professor M. Schick, and Professor O. E. Vilches for their hospitality during a visit to the University of Washington where some of these ideas were discussed. Finally, I would like to thank the University Computing Center of the University of Massachusetts for their support.

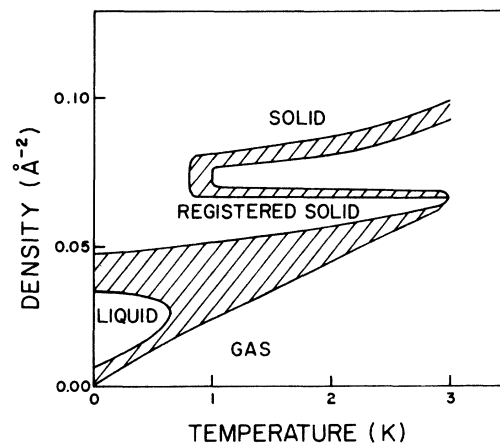


FIG. 8. Phase diagram for ^4He showing the liquid "island" and concomitant triple point. The diagonal lines fill in the coexistence regions. On this figure, only the *high*-temperature gas, the *high*-density incommensurate solid and the registered phase can be reasonable said to have been identified.

Research supported in part by the NSF under Grant No. DMR76-14447.

- ¹See, for example, G. Baym, in *The Helium Liquids, Proceedings of the Fifteenth Scottish Universities Summer School in Physics, 1974*, edited by J. G. M. Armitage and I. E. Farquhar (Academic, New York, 1975).
- ²W. J. Mullin, Phys. Rev. Lett. 20, 254 (1968); S. B. Trickey, W. B. Kirk, and E. D. Adams, Rev. Mod. Phys. 44, 668 (1972), and references cited therein.
- ³D. F. Brewer, J. Low Temp. Phys. 3, 205 (1970).
- ⁴D. C. Hickernell, E. O. McLean, and O. E. Vilches, J. Low Temp. Phys. 23, 143 (1976).
- ⁵J. G. Dash, R. F. Peierls, and M. Schick, J. Low Temp. Phys. 23, 491 (1976).
- ⁶M. Bretz, J. G. Dash, D. C. Hickernell, E. O. McLean, and O. E. Vilches, Phys. Rev. A 8, 1589 (1973).
- ⁷K. Carneiro, W. D. Ellenson, L. Passell, J. P. McTague, and H. Taub, Phys. Rev. Lett. 37, 1695 (1976).
- ⁸D. E. Hagen, A. D. Novaco, and F. J. Millford, in *Adsorption-Desorption Phenomena*, edited by F. Ricca (Academic, New York, 1972).
- ⁹H. W. Jackson, Phys. Rev. 180, 184 (1969).
- ¹⁰M. D. Miller and C.-W. Woo, Phys. Rev. A 7, 1322 (1973). Due to a numerical error the calculated specific heats were too small by a factor of 4. This correction results in reasonable agreement between theory and the experimental data of E. O. McLean [Ph.D. thesis (University of Washington, 1972) (unpublished)].
- ¹¹W. E. Massey, C.-W. Woo, and H.-T. Tan, Phys. Rev. A 2, 519 (1970).
- ¹²F. Y. Wu and E. Feenberg, Phys. Rev. 128, 943 (1962).
- ¹³C.-W. Woo, Phys. Rev. 151, 138 (1966).
- ¹⁴For a discussion of the factor-type (Van Kampen) cluster expansion see E. Feenberg, *Theory of Quantum Fluids* (Academic, New York, 1969), Chap. 8.
- ¹⁵The leading term in Σ_{44} ostensibly involves a four-particle distribution function since there are two fermion labels and two boson labels. However, since these labels enter in an "unlinked" way one can perform an extra integration to obtain a *three-body* function.
- ¹⁶M. D. Miller, C.-W. Woo, and C. E. Campbell, Phys. Rev. A 6, 1942 (1972).
- ¹⁷J. S. Rowlinson, *Liquids and Liquid Mixtures* (Academic, New York, 1959), Chap. 5.
- ¹⁸M. D. Miller, Phys. Rev. B 14, 3937 (1976).
- ¹⁹D. Schiff and L. Verlet, Phys. Rev. 160, 208 (1967).
- ²⁰A. D. Novaco and C. E. Campbell, Phys. Rev. B 11, 2525 (1975).
- ²¹G. Baym, Phys. Rev. Lett. 17, 952 (1966).
- ²²For definitions of the thermodynamic functions of mixing, see I. Prigogine, *The Molecular Theory of Solutions* (North-Holland, Amsterdam, 1957), Chap. 1.
- ²³Although this approximation for S_M would be unreasonable for the bulk liquid, it appears from Fig. 7 of HMV (where the experimental entropy of mixing is shown) that high temperature comes a good deal sooner in 2D than 3D. A word of comment on the determination of S_M by HMV is needed, however. HMV used as their fiducial system pure ^3He and ^4He at a given *density* (and temperature) which is different from the usual definition which would use pure ^3He and ^4He at a given *pressure* (see Ref. 22). They, of course, had no choice since the equation of state of the system is unknown. However, for a system like ^3He , which has an intrinsic temperature characteristic, (the Fermi temperature) it might be more appropriate to use the partial densities.
- ²⁴M. Schick and C. E. Campbell, Phys. Rev. A 2, 1591 (1970).
- ²⁵L. W. Bruch, Phys. Rev. B 13, 2873 (1976); M. D. Miller and L. H. Nosanow (unpublished).
- ²⁶S. V. Hering, S. W. Van Sciver, and O. E. Vilches, J. Low Temp. Phys. 25, 793 (1976).